Hindawi Publishing Corporation
Journal of Sensors
Volume 2013, Article ID 624981, 5 pages
http://dx.doi.org/10.1155/2013/624981

Research Article

A Tent Map Based A/D Conversion Circuit for Robot Tactile Sensor

Jianxin Liu,[1] Xuan Zhang,[2] Zhiming Li,[2] and Xuling Li[2]

[1] *NARI Technology Development Limited Company, Nanjing 210061, China*
[2] *Experiment & Verification Center, State Grid Electric Power Research Institute, Nanjing 210061, China*

Correspondence should be addressed to Xuan Zhang; sherry.zhangxuan@gmail.com

Received 10 July 2013; Accepted 25 July 2013

Academic Editor: Aiguo Song

Force and tactile sensors are basic elements for robot perception and control, which call for large range and high-accuracy amplifier. In this paper, a novel A/D conversion circuit for array tactile sensor is proposed by using nonlinear tent map phenomenon, which is characterized by sensitivity to small signal and nonlinear amplifying function. The tent map based A/D conversion circuits can simultaneously realize amplifying and A/D converting functions. The proposed circuit is not only simple but also easy to integrate and produce. It is very suited for multipath signal parallel sampling and A/D converting of large array tactile sensor.

1. Introduction

In recent decades, with the rapidly development of robot technology, robot sensors have received much attention as a sensing element for robot. Multiaxis force sensors and array tactile sensors, usually called haptic sensors, especially, have become the major research content in the robot sensor research areas [1, 2]. People hope that robot haptic sensor can be like human perception organs which have high measurement accuracy, with similar hand force and tactile organ of integration, miniaturization, and flexibility characteristics. For instance, Song developed a small four-degree-of-freedom wrist force sensor with high precision, which consists of small cross-elastic beam, compliant beams, and the base of the elastic body. It is a kind of self-decoupling force sensor in mechanical structure [3]. Beyeler et al. designed a six-axis MEMS force sensor with a movable body suspended by flexures which allow deflections and rotations along the x-, y-, and z-axes. And the orientation of this movable body is sensed by seven capacitors based on transverse sensing, resulting in a high sensitivity [4]. Ma et al. proposed a novel nonlinear static decoupling algorithm based on the establishment of a coupling error model for 3-axis force sensor in order to avoid overfitting and minimize the negative effect of random noises in calibration data, which can obtain high precise measurement results of 3-axis force for robot force control [5]. Although robot array tactile sensor can be regarded as a multipoint integrated force sensor, due to flexible and miniaturization requirements of tactile sensor which are high, the measurement principle is more complex than the multiaxis force sensor [6, 7]. Song et al. proposed a novel design of a haptic texture sensor by using PVDF film to fabricate a high-accuracy, high-speed-response texture sensor [8]. Lee and Won developed a novel tactile imaging sensor by using a multilayer polydimethylsiloxane optical waveguide as the sensing probe, which is capable of measuring the elasticity of the touched object with high precision [9]. Based on semiconductor technique, piezoresistive, capacitive, piezoelectric, and other types of robot, array tactile sensors are developing rapidly. Array tactile sensors have a corresponding increase in array size and resolution [10, 11]. Nonetheless, because of measurement mechanism limit, output signal of sensing element of most high-resolution tactile sensors is relatively weak. In addition, as the expansion of tactile array, it hopes that tactile image signal has a fast A/D conversion rate. Sharing the same A/D conversion in small scale tactile sensor cannot meet the real-time requirements of signal acquisition for the large scale array tactile sensor.

In recent years, some of the unique properties of nonlinear systems have much in measurement area for their unique

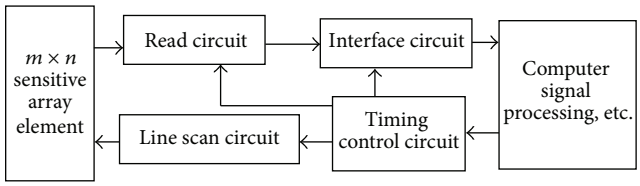

Figure 1: Tactile sensor array signal acquisition circuit.

character, such as the chaotic system sensitivity to small signal [12], nonlinear mapping [13], nonlinear information storage [14], and resonance stochastic [15]. In this paper, a tent map is sensitive to small signal circuit and nonlinear transform of unique properties. A novel A/D conversion circuit for robot tactile sensor array is proposed to achieve parallel sampling of multichannel tactile signals and A/D conversion with high cost performance, which has a conditioning amplification and A/D conversion function integration advantages in combination, simple circuit, and easy integration to realize.

2. Signal Acquisition System for Robot Tactile Sensor

Typical signal acquisition circuit for robot tactile sensor is shown in Figure 1, including timing control circuit, line scan circuit, read circuit, and interface circuit. The whole signal acquisition process was controlled and coordinated by timing control circuit. According to the arrangements of the timing control circuit, line scan circuit is ordered in m clock cycles to send the periodic excitation signal to m-line array sensitive element, while the read circuit is ordered in m clock cycles to read the output signal of n column in parallel. Then through interface circuit which consists of signal conditioning and A/D conversion, tactile signals were transferred to the computer for processing and target recognition.

Conventional robot array tactile sensor, because of the small array size (about 8×8), often uses an A/D conversion in order to complete the analog-digital conversion of output signal of $m \times n$ sensitive elements.

3. Small Signal Nonlinear Amplifier and A/D Conversion Based on Tent Map

Tent map was a typical one-dimensional chaotic system [16], which was described as

$$x_{n+1} = T(x_n) = \begin{cases} 2x_n, & 0 < x_n \le 0.5, \\ 2(1 - x_n), & 0.5 < x_n < 1, \end{cases} \quad (1)$$

where $x_n \in [0, 1]$, $n = 0, 1, 2, \ldots$.

This map consisted of two steps: the first step was to uniformly elongate the interval $[0, 1]$ to its doubled range; the second step was to fold the elongated interval into the original interval $[0, 1]$. These iterative operations would cause the separation of adjacent points index, eventually to achieve the state of chaos.

Tent map on the initial value (the system input signal) amplification was different from the linear amplification method. Linear amplification multiples were a constant and also limited by system operating range. Tent map system in chaotic state amplified the signal doubly and folded the doubled range symmetrically in each iteration, so that the initial small signal could eventually be greatly amplified without beyond range of system operating after several iterations.

The initial value x_0, which was corresponding to the input signal of tent map system V_{in}, could be described as a binary fraction

$$x_0 = 0.t_0 t_1 t_2 \cdots = \sum_{j=0}^{\infty} \frac{t_j}{2^{j+1}}. \quad (2)$$

In order to obtain the relationship of the iterative output and the initial signal of discrete tent map, here, this paper would introduce the nonlinear relationship of Bernoulli shift; its kinetic equation was

$$x'_{n+1} = B(x'_n) = \begin{cases} 2x'_n, & 0 < x'_n \le 0.5, \\ 2x'_n - 1, & 0.5 < x'_n < 1. \end{cases} \quad (3)$$

In each iteration, Bernoulli shift left shifted the binary fraction $t_1, t_2, \ldots$ one place

$$\begin{aligned} x'_1 &= B(x'_0) = 0.t_1 t_2 t_3 \cdots, \\ x'_2 &= B(x'_1) = 0.t_2 t_3 t_4 \cdots. \end{aligned} \quad (4)$$

For Bernoulli shift, $b_n = \text{sgn}(x'_n - 0.5)$ was defined as the nth iteration output; there $b_n = t_n$, and b_i, $i = 0, 1, 2, \ldots$, was a binary sequence. For tent map, if we define $g_n = \text{sgn}(x_n - 0.5)$, then the corresponding relationship between g_i, $i = 0, 1, 2, \ldots$, and b_i, $i = 0, 1, 2, \ldots$, was as follows:

(1) when $0 < x_k < 0.25$, that is, $b_k = 0$, then $B(x_k) < 0.5$, $b_{k+1} = 0, T(x_k) < 0.5$, and $g_{k+1} = 0$;

(2) when $0.25 < x_k < 0.5$, that is, $b_k = 0$, then $B(x_k) > 0.5, b_{k+1} = 1, T(x_k) > 0.5$, and $g_{k+1} = 1$;

(3) when $0.5 < x_k < 0.75$, that is, $b_k = 1$, then $B(x_k) < 0.5, b_{k+1} = 0, T(x_k) > 0.5$, and $g_{k+1} = 1$;

(4) when $0.75 < x_k < 1$, that is, $b_k = 1$, then $B(x_k) > 0.5, b_{k+1} = 1, T(x_k) < 0.5$, and $g_{k+1} = 0$.

Therefore, g_i, $i = 0, 1, 2, \ldots$, was a Gray-code sequence of b_i, $i = 0, 1, 2, \ldots$:

$$g_{k+1} = b_k \oplus b_{k+1}, \quad k = 0, 1, 2, \ldots. \quad (5)$$

According to the above formula and initial time $x_0 = x'_0 = V_{\text{in}}$, we could obtain

$$\begin{aligned} b_{k+1} &= b_k \oplus g_{k+1}, \quad k = 0, 1, 2, \ldots, \\ b_0 &= g_0. \end{aligned} \quad (6)$$

So we designed a tent map iteration output Gray-code sequence g_i, $i = 0, 1, 2, \ldots$, into a binary sequence of Bernoulli

Table 1: Results of the A/D conversion.

Sensitive element	(8, 1)	(8, 2)	(8, 3)	(8, 4)	(8, 5)	(8, 6)	(8, 7)	(8, 8)
Output value (mV)	0	0	0	0	25	80	188	246
Gray code $g_0g_1g_2g_3g_4g_5g_6g_7$	00000000	00000000	00000000	00000000	00000101	00011111	00101000	00100001
Binary code $b_0b_1b_2b_3b_4b_5b_6b_7$	00000000	00000000	00000000	00000000	00000110	00010101	00110000	00111110
Calculated value (mV)	0.0	0.0	0.0	0.0	23.4	82.0	187.5	242.2
Sensitive element	(8, 9)	(8, 10)	(8, 11)	(8, 12)	(8, 13)	(8, 14)	(8, 15)	(8, 16)
Output value (mV)	310	230	170	67	33	0	0	0
Gray code $g_0g_1g_2g_3g_4g_5g_6g_7$	01101000	00100111	00111110	00011001	00001100	00000000	00000000	00000000
Binary code $b_0b_1b_2b_3b_4b_5b_6b_7$	01001111	00111010	00101011	00010001	00001000	00000000	00000000	00000000
Calculated value (mV)	308.5	226.5	168.0	66.4	31.3	0.0	0.0	0.0

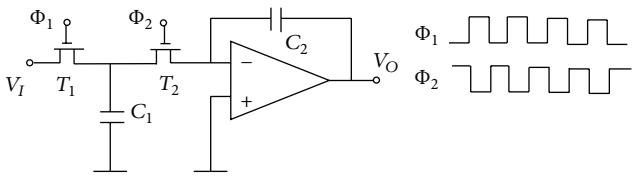

Figure 2: Switched capacitor integral circuit.

map b_i, $i = 0, 1, 2, \ldots$, and then calculated the initial value through binary fraction sequence as follows:

$$x_0 = \sum_{j=0}^{N} \frac{b_j}{2^{j+1}}, \tag{7}$$

where g_i, $i = 0, 1, 2, \ldots$, was the needed digital value. Here, tent map completed signal amplification and A/D conversion function.

4. Implementation on the Circuit of Tent Map for A/D Conversion

A/D circuit basic element was switched capacitor integral circuit shown in Figure 2, where T_1 and T_2 were analog switches and C_1 and C_2 were capacitors. The clocks Φ_1, Φ_2 were in reverse phase with same period T. During the former half period of T, the T_1 was on and T_2 was off; thus the C_1 was charged by input voltage V_I. During the latter half period of T, T_1 was off and T_2 was on, so that the C_2 was charged by C_1V_I. The output voltage of this circuit in a period was

$$V_o(nt) = V_o((n-1)t) - \frac{C_1}{C_2}V_I((n-1)t). \tag{8}$$

The tent map circuit consisted of the above circuit as shown in Figure 3. Parts I and III implemented the function of $y = 2x$, and parts II and III implemented the function of $y = 2(1 - x)$. Part IV was a circuit for holding and delay.

Figure 4 shows the control logic for A/D conversion. First, start signal got high, and switch J_0 connected the input signal with the part I and part II. After delay of t_1, D trigger produces a switch instruction; if $0 \le V_i \le 0.5$, then J_1 was switched on; if $0.5 < V_i < 1$, then J_2 was switched on. At time $t_1 + t_2$, the control signal e switches were high, so that the charge of C_1 or C_2 was transferred to C_3, due to $C_3 = (1/2)C_1 = (1/2)C_2$, so that the input voltage was amplified doubly. In the meantime, C_4 was also charged. At the next time 0, the o switches were switched off and e switches were switched on, so that the charge of C_4 was transferred to C_5 and results in $V_{C_5} = V_{C_4}$. At the same time, J_0 was disconnected with input signal V_0, so that an iterative feedback loop exists in the A/D conversion, and C_1, C_2 were charged by the same feedback voltage to realize $y = 2x$ and $y = 2(1 - x)$. This circle continuously iterated N times.

Hence the N binary bits output of D trigger was the Gray-code sequence of A/D conversion

$$\begin{aligned} g_k &= \overline{Q}_k \quad (k = 1, 2, 3, \ldots), \\ b_0 &= Q_0. \end{aligned} \tag{9}$$

The above g_k sequence, the initial condition $b_0 = Q_0$ into (6), and Bernoulli binary sequence b_k $(k = 0, 1, 2, \ldots)$ could be obtained.

5. Array Tactile Sensor Signal Acquisition System Based on Tent Map of A/D Circuit

The schematic diagram of signal amplification of array tactile sensor analog and A/D conversion based on tent map circuit is shown in Figure 5. According to the arrangements of the timing control circuit, line scan circuit sent the periodic excitation signal to m-line array sensitive element, while the read circuit read the output signal of n column in parallel. The n-column signal was generated by simultaneously signaling nonlinear amplification and analog-digital conversion of n of A/D converters based on tent map. The resulting Gray-code sequence was sent directly to the computer which will

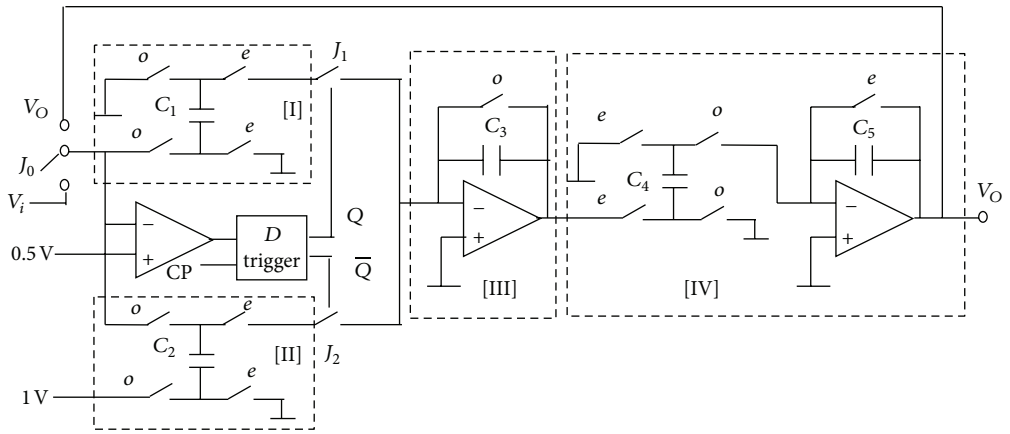

Figure 3: The circuit of tent map for A/D conversion.

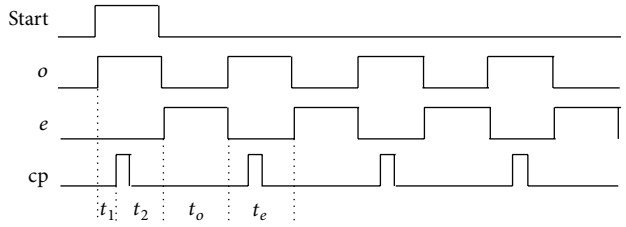

Figure 4: Circuit logic for the A/D conversion.

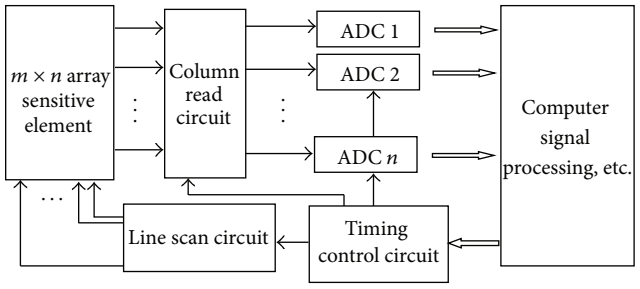

Figure 5: The schematic diagram of array tactile sensor signal acquisition system based on tent map of A/D circuit.

complete the conversion of Gray code to binary code. Then, under the control of timing logic, the read n-column signal on the next line, and the completed amplification and A/D conversion, after obtaining an $m \times n$ tactile image signal by the computer, we could process tactile signals.

We could carry out the amplification and A/D conversion experiments sensitive element signal of 16×16 microarray tactile sensor based on the above circuit. The results of the A/D conversion for eight sensitive elements in the 8th line were shown in Table 1, which indicates that A/D circuits based on the tent map could effectively achieve the amplification and A/D conversion of a small signal.

Figure 6 is the output of a 16×16 micro array tactile sensor manufactured by us based on the tent map circuit when a very light hexagon aluminum flake was put on it. The measurement range of each tactile sensing unit was from 0.01 N to 10 N, which shows that the proposed tent map

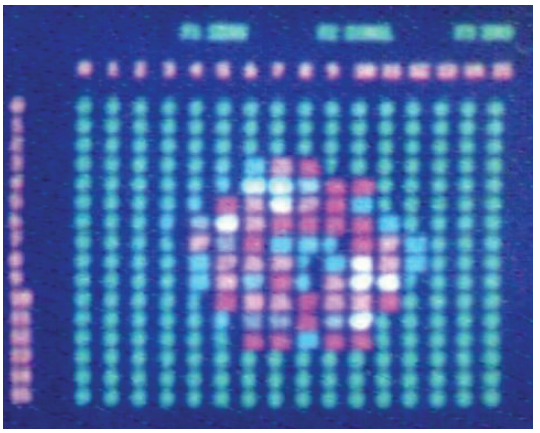

Figure 6: The output of a 16×16 array tactile sensor based on the tent map circuit when a very light hexagon aluminum flake was put on it.

based A/D conversion circuits had the advantages of large amplification range and high resolution. By comparison with the conventional high precision array tactile sensor [17], our method is more cost effective and easier to realize.

6. Conclusion

This paper presents a novel A/D conversion circuit for robot array tactile sensor of unique properties. The circuit makes use of unique advantage for tent map sensitive to small signal circuit and nonlinear transform and has conditioning amplification and A/D conversion function integration advantages, simple circuit, and easy integration to realize. This method can achieve the parallel sampling of multichannel tactile signal and A/D converter, which can meet the real-time requirements of signal acquisition for the large scale array tactile sensor. This experiment gives the effectiveness of this method.

Acknowledgments

This work was supported by the Science and Technology Project of National Energy Administration (no. NY20110702-1)

and the Technology Project of State Grid Corporation of China in 2013-2014 (project name is Study of Testing and Detection Technology for Electric Vehicle Charging and Battery Swap Infrastructure).

References

[1] H. Yousef, M. Boukallel, and K. Althoefer, "Tactile sensing for dexterous in-hand manipulation in robotics—a review," *Sensors and Actuators A*, vol. 167, no. 2, pp. 171–187, 2011.

[2] J. Ma and A. Song, "Fast estimation of strains for cross-beams six-axis force/torque sensors by mechanical modeling," *Sensors*, vol. 13, no. 5, pp. 6669–6686, 2013.

[3] A. Song, J. Wu, G. Qin, and W. Huang, "A novel self-decoupled four degree-of-freedom wrist force/torque sensor," *Measuremen*, vol. 40, no. 9-10, pp. 883–891, 2007.

[4] F. Beyeler, S. Muntwyler, and B. J. Nelson, "A six-axis MEMS force-torque sensor with micro-Newton and nano-Newton-meter resolution," *Journal of Microelectromechanical Systems*, vol. 18, no. 2, pp. 433–441, 2009.

[5] J. Ma, A. Song, and J. Xiao, "A robust static decoupling algorithm for 3-axis force sensors based on coupling error model and ε-SVR," *Sensors*, vol. 12, no. 11, pp. 14537–14555, 2012.

[6] J.-H. Kim, J.-I. Lee, H.-J. Lee, Y.-K. Park, M.-S. Kim, and D.-I. Kang, "Design of flexible tactile sensor based on three-component force and its," in *Proceedings of the IEEE International Conference on Robotics and Automation*, pp. 2578–2581, April 2005.

[7] M. H. Lee and H. R. Nicholls, "Tactile sensing for mechatronics—a state of the art survey," *Mechatronics*, vol. 9, no. 1, pp. 1–31, 1999.

[8] A. Song, Y. Han, H. Hu, L. Tian, and J. Wu, "Active perception-based haptic texture sensor," *Sensors and Materials*, vol. 25, no. 1, pp. 1–15, 2013.

[9] J.-H. Lee and C.-H. Won, "High-resolution tactile imaging sensor using total internal reflection and nonrigid pattern matching algorithm," *IEEE Sensors Journal*, vol. 11, no. 9, pp. 2084–2093, 2011.

[10] J. Dargahi and S. Najarian, "Advances in tactile sensors design/manufacturing and its impact on robotics applications—a review," *Industrial Robot*, vol. 32, no. 3, pp. 268–281, 2005.

[11] S. Saga, H. Kajimoto, and S. Tachi, "High-resolution tactile sensor using the deformation of a reflection image," *Sensor Review*, vol. 27, no. 1, pp. 35–42, 2007.

[12] N. Singh and A. Sinha, "Chaos-based secure communication system using logistic map," *Optics and Lasers in Engineering*, vol. 48, no. 3, pp. 398–404, 2010.

[13] L. Zhang, A. Song, and J. He, "Stochastic resonance of a subdiffusive bistable system driven by Lévy noise based on the subordination process," *Journal of Physics A*, vol. 42, no. 47, Article ID 475003, 2009.

[14] A. Song, J. Duan, J. Wu, and H. Li, "Design 2D nonlinear system for information storage," *Chaos, Solitons and Fractals*, vol. 41, no. 1, pp. 157–163, 2009.

[15] D. Rousseau, J. R. Varela, and F. Chapeau-Blondeau, "Stochastic resonance for nonlinear sensors with saturation," *Physical Review E*, vol. 67, no. 2, Article ID 021102, 6 pages, 2003.

[16] X. Yi, "Hash function based on chaotic tent maps," *IEEE Transactions on Circuits and Systems II*, vol. 52, no. 6, pp. 354–357, 2005.

[17] H.-K. Kim, S. Lee, and K.-S. Yun, "Capacitive tactile sensor array for touch screen application," *Sensors and Actuators A*, vol. 165, no. 1, pp. 2–7, 2011.